

1 Article

2 A Novel Method of Synthesizing Graphene for 3 Electronic Device Applications

4 Nierlly Galvão^{1,*}, Getulio Vasconcelos², Rodrigo Pessoa^{1,3,*}, João Machado⁴, Marciel Guerino¹,
5 Mariana Fraga³, Bruno Rodrigues^{1,3}, Julien Camus⁵, Mohamed Djouadi⁵ and Homero Maciel^{1,3}

6 ¹ Centro de Ciência e Tecnologia de Plasmas e Materiais – PlasMat, Instituto Tecnológico de Aeronáutica,
7 12228-900, São José dos Campos, SP, Brazil.

8 ² Photonics Division, Instituto de Estudos Avançados, Rodovia dos Tamoios, 12228-001, São Jose dos
9 Campos, SP, Brazil.

10 ³ Universidade Brasil, Rua Carolina Fonseca 235, 08230-030, São Paulo, SP, Brazil.

11 ⁴ Associate Laboratory of Sensors and Materials, Instituto Nacional de Pesquisas Espaciais, 12227-010, São
12 José dos Campos, SP, Brazil.

13 ⁵ Institut des Matériaux Jean Rouxel IMN, UMR 6502, Université de Nantes, 2 rue de La Houssinière, BP
14 32229, 44322 Nantes Cedex, France.

15 * Correspondence: nierlly@gmail.com (N.G.); rspessoa@ita.br (R.P.); Tel.: +55-012-3947-6882 (N.G.); +55-012-
16 3947-5942 (R.P.)

17

18 **Abstract:** This article reports a novel and efficient method to synthesize graphene by thermal
19 decomposition process. In this method, silicon carbide (SiC) thin films grown on Si(100) wafers with
20 an AlN buffer layer were used as substrates. A CO₂ laser beam heating without vacuum or
21 controlled atmosphere was applied for SiC thermal decomposition. The physical, chemical,
22 morphological, and electrical properties of the laser-produced graphene were investigated for
23 different laser energy densities. The results demonstrate that graphene was produced in form of
24 small islands with quality, density and properties depending on the applied laser energy density.
25 Furthermore, the produced graphene exhibits a sheet resistance characteristic similar to graphene
26 grown on mono-crystalline SiC wafer, which indicates its potential for electronic device
27 applications.

28 **Keywords:** graphene synthesis; silicon carbide; thin film; high-power impulse magnetron
29 sputtering; thermal decomposition, electronic devices.

30

31 1. Introduction

32 Nowadays, the synthesis of high-quality graphene has been the focus of several researches due
33 to great potential applications of this material, as for example in electronic devices, sensors and
34 flexible displays [1]. Among the graphene synthesis methods, the thermal decomposition processes
35 have been successful used to grow graphene layers on silicon carbide (SiC) [2-5]. In general, these
36 studies show the use of SiC wafers as substrates to be decomposed by heating using an induction
37 furnace at vacuum or at atmospheric pressure with an inert gas flow [6-10]. The kinetics of graphene
38 formation and properties, such as structure and morphology, show to be dependent on the reactor
39 pressure, type of gas atmosphere, orientation and face termination of the SiC wafer [10-12].

40 Most recently, the use of a laser beam as heating source for graphene formation from SiC has
41 been reported [13-15]. The focus of these studies was to investigate the growth of graphene on Si-
42 and/or C-face of SiC wafers termination. Perrone et al. used a near infrared Nd:YVO₄ (1064 nm) laser
43 to promote the heating of SiC surface [13]. They reported a possible presence of graphene when
44 process was performed using an argon flow or vacuum at a pressure of 10⁻⁵ Torr. Using ultra-high
45 vacuum (UHV), only a disordered graphite phase was observed [13]. Lee et al. using an UV laser (248
46 nm) noticed not only that it is possible to grow epitaxial graphene (EG) from Si-terminated SiC (0001),

47 as pointed out that EG has a structure comparable to thermally grown graphene in UHV using the
48 same substrate [14]. Unlike the previous two works, Yannopoulos et al. obtained graphene on SiC
49 without the use of vacuum environment or pre-treatment of SiC substrate [15]. In their work, a carbon
50 dioxide (CO₂) laser beam was used as the heating source and the argon gas flow at atmospheric
51 pressure was applied to form few layers of EG. An advantage of the use of CO₂ laser is the cooling
52 effect during pulse and the possibility of writing graphene patterns on SiC, which eliminates the
53 lithographic step [15]. Nevertheless, the aforementioned studies and processes have a serious
54 drawback that is the use of high-cost SiC wafers as substrate [16, 17].

55 In other recent study, Galvão et al. reported on the growth of graphene layers on a low cost
56 polycrystalline SiC substrate obtained from powder metallurgy using a CO₂ laser beam [18].
57 Although the graphene obtained may be applied in several areas, the SiC substrate is not ideal for
58 microelectronic applications. In order to improve the quality of the graphene samples without
59 significant increase in the production costs, we explore the use of SiC thin films as substrates in
60 combination with the CO₂ laser beam heating technique for EG growth. Herein, SiC thin films were
61 grown by high-power impulse magnetron sputtering (HiPIMS) on silicon substrates covered with an
62 aluminum nitride (AlN) buffer layer. To the best of our knowledge, the formation of graphene from
63 SiC thin films grown on AlN/Si substrates using CO₂ laser beam has not yet been reported in literature
64 [19]. In this work, different levels of laser energy density were applied during SiC thermal
65 decomposition and the chemical properties and quality of the graphene were evaluated using Raman
66 spectroscopy. Moreover, to further understand the material characteristics, morphological and
67 electrical properties of the samples were investigated using AFM and four points probe method,
68 respectively.

69 2. Materials and Methods

70 2.1. SiC thin film growth

71 SiC thin films were deposited by HiPIMS technique on pieces of polished p-type Si(100) wafer
72 covered with AlN buffer in a high-vacuum chamber with a background pressure of 6×10^{-6} Torr. More
73 details of the magnetron sputtering system can be found elsewhere [19]. The working pressure of the
74 argon gas (99.999%) was maintained at 3×10^{-3} Torr for a corresponding flow rate of 20 sccm. A high-
75 purity SiC (99.5%, Kurt J. Lesker) target with a 4-inch diameter was used. The sputtering reactor was
76 powered by a HiPIMS power supply (Solvix HIP³ 5kW) with an applied power of 200 W and duty
77 cycle of 5%. The target-to-substrate distance was approximately 65 mm and the deposition was
78 performed during 10 min. The substrate holder was in a floating potential. Before starting the SiC
79 deposition, a pre-sputtering period (10 min, at 200 W) was performed to remove the contamination
80 from the target surface. The obtained SiC film on AlN/Si substrate had an average thickness around
81 240 nm.

82 The AlN buffer layer was grown on the Si(100) substrates using the HiPIMS technique at
83 "Institut des Matériaux Jean Rouxel in Nantes University". More details can be found elsewhere [20,
84 21]. The AlN film on Si substrate had an average thickness around 1300 nm and the main
85 crystallographic orientation was (002).

86 87 2.2. SiC sublimation by CO₂ laser heating

88 The heating of the SiC thin film was carried out by using a CO₂ laser (Synrad Evolution – 125)
89 with a beam diameter of 200 μm , which emits infrared laser radiation at a wavelength band of 10.6
90 μm . The samples were positioned at 5 mm below the laser focal point (see schematic diagram of the
91 laser irradiation process in [18]). For all the processes, a beam overlap of 50% was used. Three
92 different laser scanning velocity rates were used: 2300, 2500 and 2600 mm s^{-1} . For all conditions, the
93 laser power applied was 50 W, which corresponded to 40% of the overall power. The entire process
94 occurred under ambient atmosphere and pressure conditions. The energy densities of each scanning
95 velocity were calculated and are shown in Table 1. One can note that in this investigation the energy
96 densities were between 127-145 J cm^{-2} , whereas in the previous works the values were between 132-
97 200 J cm^{-2} [18]. The choice of a lower energy density range is due to the properties of the synthesized

98 graphene at higher laser energy density did not present significant difference in comparison with
 99 samples produced with lower energy density [18].
 100

101 **Table 1.** Scanning velocities and energy densities applied for each condition.

	Condition 1 (C1)	Condition 2 (C2)	Condition 3 (C3)
Scanning velocity (mm s ⁻¹)	2300	2500	2600
Energy density (J cm ⁻²)	145.25	136.95	127.69

102

103 2.3. Material characterization

104 The structure of the as-deposited SiC films was investigated using Grazing Incidence XRD with
 105 an incidence angle (ω) of 0.3° operated with a PANalytical X'pert Pro x-ray diffractometer with CuK α
 106 radiation.

107 Raman analyses were performed using a Horiba Raman microprobe system equipped with an
 108 argon ion laser (514.5 nm). Raman spectra of the SiC and graphene samples were obtained at room
 109 temperature in the range of 200 to 1100 cm⁻¹ and 1200 to 2900 cm⁻¹, respectively. The Raman spectral
 110 imaging or Raman mapping were obtained focusing on the main characteristic bands (or peaks) of
 111 graphene. The type of the defects presented in the graphene film was inferred according to Eckmann
 112 et al. [22], which reported on a relation between the intensity (height) of the ID and ID' peaks with
 113 the type of defect present in the graphene sample. The maximum ID/ID' ratio (~13) would correspond
 114 to sp³-defects, (~7) for vacancy-like defects and, (~3.5) for boundaries defects [22]. In this work, the D'
 115 peak is merged with the G peak. To determine the intensity of D' peak, a Lorentzian double peaks
 116 function fitting was applied to each Raman spectrum.

117 The surface morphology was investigated by atomic force microscopy (AFM Veeco Multimode
 118 with Nanoscope V control station). The tapping mode was used for all samples except for sample C2,
 119 where contact mode was applied because it provided images with better resolutions.

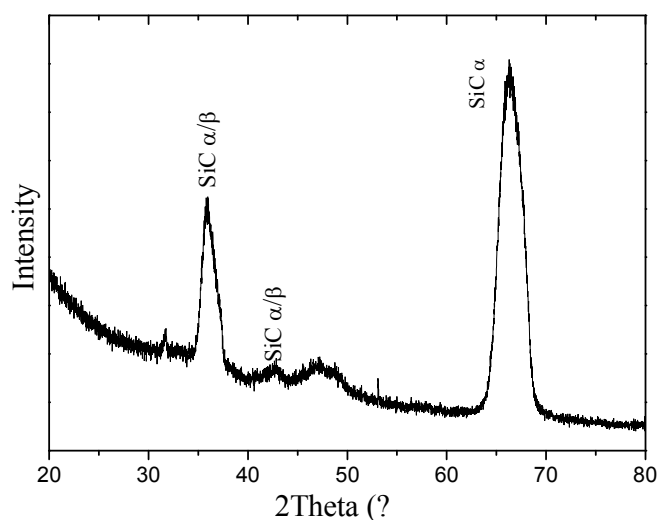
120 3. Results and Discussion

121 3.1. SiC thin film structure

122

123 In the literature, there is only one report about the SiC growth on Si substrate using the HiPIMS
 124 technique [23]. However, due to the large mismatch between SiC and Si (~ 20%), the grown film
 125 exhibited an amorphous characteristic and a high residual stress [23, 24]. To reduce these effects,
 126 several studies have demonstrated that using a sacrificial layer (buffer layer) on Si substrate before
 127 the deposition of SiC is an effective alternative. In this work, we chose to use the AlN buffer, which
 128 presents a mismatching in the lattice constant of less than 1% comparing to SiC. Figure 1 shows the
 129 GIXRD spectrum of the SiC thin film grown on AlN/Si(100) substrate. As expected, the identified
 130 peaks reveal the polycrystalline nature of the SiC.

131 In addition, the orientations of SiC indicated in GIXRD spectrum is in agreement with some
 132 studies in the literature [25-27]. We found that the peaks of the SiC matched well with those of α -SiC
 133 (6H-SiC), however, it can be not excluded that the existence of β -SiC (3C-SiC).

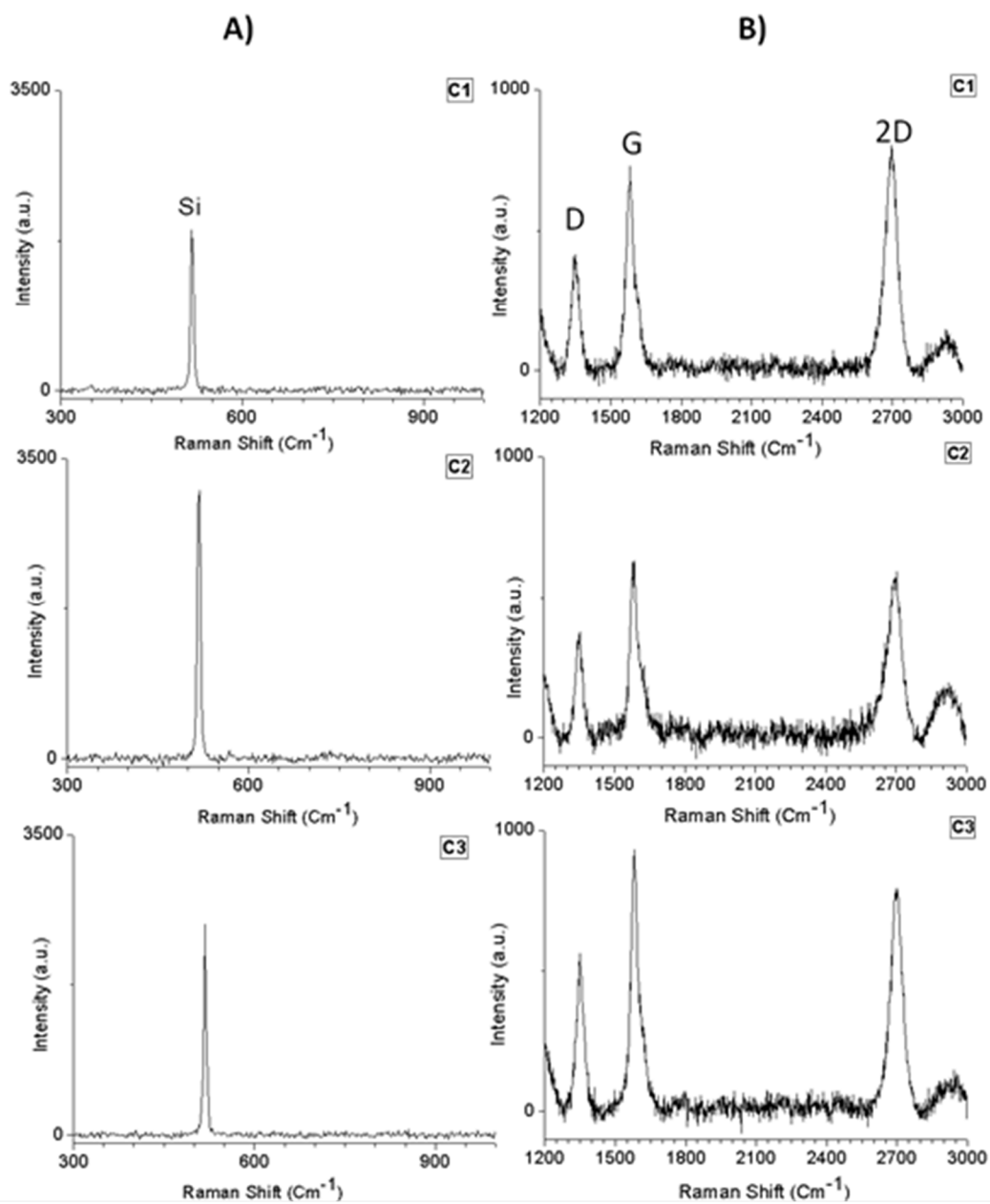


134
135 **Figure 1.** Grazing incidence XRD spectrum of SiC film grown on AlN/Si(100) substrate.
136

137 *3.2. Graphene characterization*

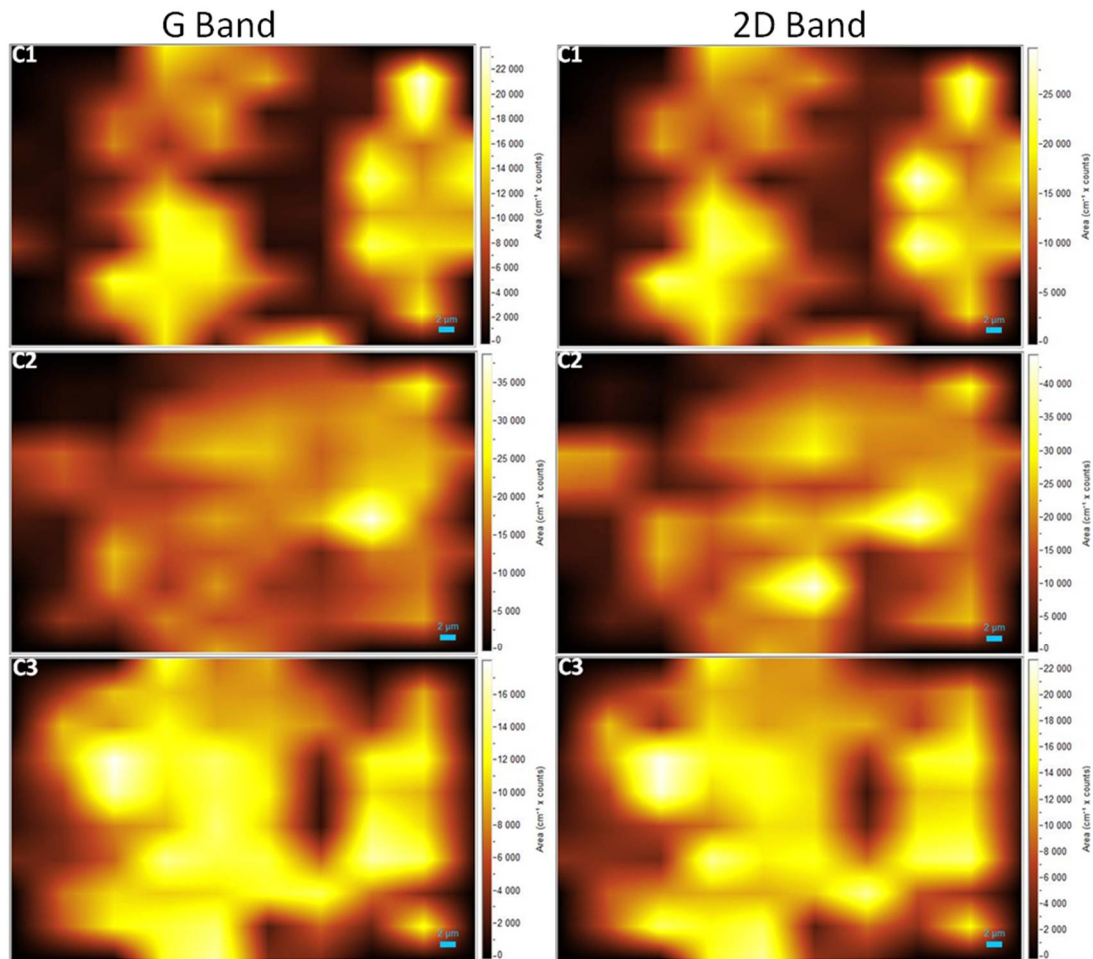
138 Raman spectroscopy is a very useful technique to obtain important information about inherent
139 features of carbon materials, such as graphene [28-31]. The Raman spectra of the graphene contain
140 three main in-plane vibrational bands: (i) G-band ($\sim 1584\text{ cm}^{-1}$), corresponding to the doubly
141 degenerate E_{2g} phonon mode at the Brillouin zone center; (ii) D-band ($1200\text{-}1400\text{ cm}^{-1}$) that arises from
142 TO phonons around the K point and requires a defect for its activation; and (ii) 2D-band ($2400\text{-}2800$
143 cm^{-1}), that is the second order of the D-band and has been widely used to evaluate the number of
144 layers and structural quality of graphene [28, 32].

145 Figure 2 shows the Raman spectra of each SiC sample that was laser treated. In addition, the
146 Raman spectra of the unexposed SiC area are also presented. The presence of graphene G and 2D-
147 bands and a significant amount of defects (D-band) is observed (Figure 2b). Conversely, we notice
148 the absence of peaks related to the Si-C band (Figure 2a). The absence of the Si-C bands can be an
149 indication that, at this point, all the SiC was decomposed to form graphene. To verify the growth
150 behavior and distribution of graphene in the treated sample, a Raman mapping was performed
151 (Figures 3 and 4).
152



153
154
155
156

Figure 2. Raman spectra of the samples C1, C2 and C3: (a) scanning in the SiC area (column A); (b) scanning in the graphene area (column B).

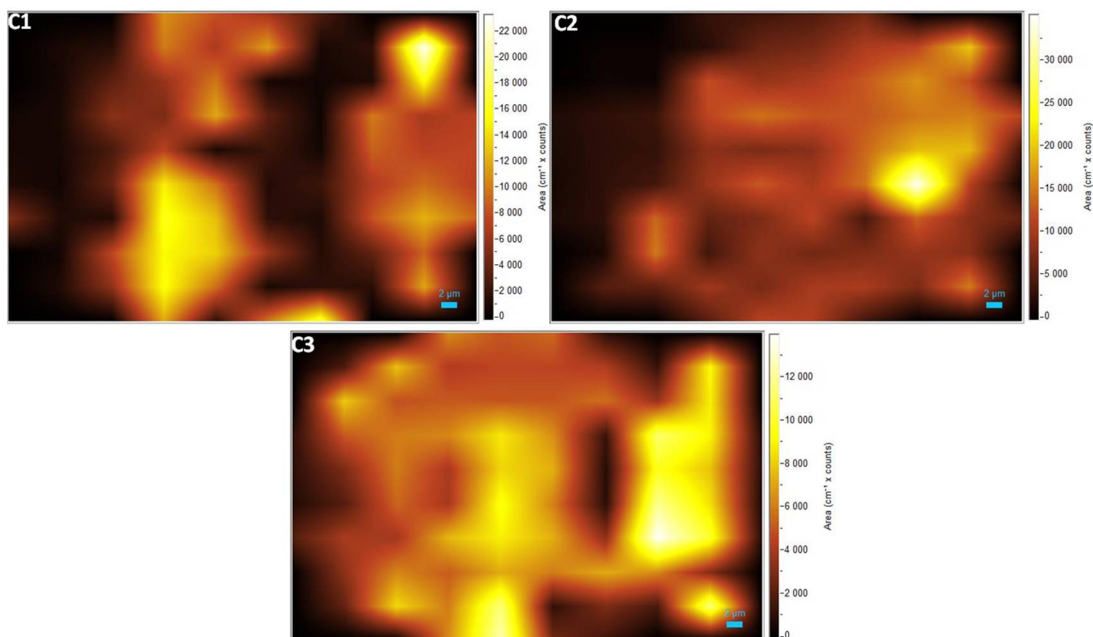


157

158

159

Figure 3. Raman mapping of the samples corresponding to G and 2D bands.



160

161

162

163

164

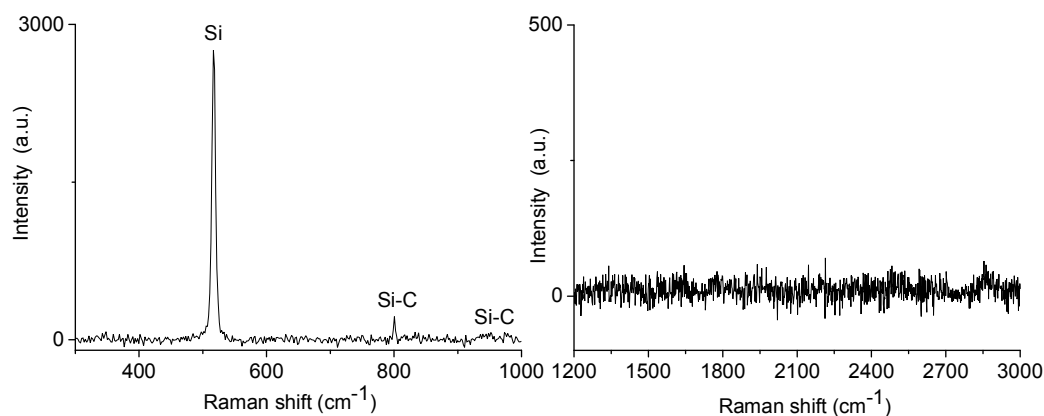
Figure 4. Raman mapping of the samples corresponding to D band.

The bright spots observed in the Raman maps (Figures 3 and 4), which are due to the presence of bands related to graphene, are in agreement with the Raman spectra shown in Figure 2. The dark

165 areas correspond to the absence of bands related to graphene. The mapping images also reveal that
166 graphene did not expand enough to cover the entire region of analysis, forming some “graphene
167 islands”. Furthermore, it is possible to observe a non-uniform distribution of higher intensity regions.
168 This variation is probably related to the quality of graphene. Several studies reported that the kinetics
169 of graphene growth on Si- or C-face of SiC is distinct [3, 32, 33, 34]. When EG is grown on the Si-face
170 in the UHV environment, the rate of sublimation is reduced and therefore it is possible to control the
171 growth of graphene layers. This leads to a large and homogeneous monolayer [36, 37].

172 When the C-face is considered, the growth rate is higher, and its control is more difficult, which
173 usually results in an inhomogeneous graphene [3, 33, 34]. However, Hass et al. reported that
174 graphene grown on C-face of the SiC substrate, in a RF furnace, can present an exceptional quality
175 [37]. This indicates that depending on the technique it is possible to obtain good quality graphene on
176 both faces. In our studies, graphene was grown on SiC thin film with undefined face-termination (Si-
177 C face). Currently, there is a clear lack of studies reporting on the kinetics of graphene growth on SiC
178 thin films using thermal decomposition by CO₂ laser heating. Thus, according to the behavior
179 observed in Raman mapping and considering that the SiC film is polycrystalline and contains some
180 amorphous areas, it is possible to presume that graphene was grown from both Si-C face
181 terminations. These two possible faces growth can result in graphene regions with high defect
182 concentration and different layers. In addition, the laser heating may also have influenced the growth
183 and quality of graphene. As obtained by Galvão et al. [18], the limited growth of graphene and non-
184 dissociation of SiC in some regions of the material may have been influenced by the heat transfer
185 along and across the heterogeneous surface. Inhomogeneities on the surface cause a non-uniform
186 temperature distribution. A detailed Raman analysis performed on sample C2 revealed that the dark
187 areas on the maps are composed by SiC films that did not get enough energy to dissociate and form
188 graphene; however, crystallization started to take part instead, which can be verified by the well-
189 defined SiC peak showed in Figure 5.

190



191

192

193 **Figure 5.** Raman spectra of the dark areas for C2 sample: (a) scanning in the SiC range (column
194 A); (b) scanning in the Graphene range (column B).

195 3.3. Sheet resistance and morphology of SiC thin film and graphene layers

196 As graphene is a material of great interest for electronic device applications, we have also
197 analyzed the sheet resistance for each sample (Table 2) produced by the developed method. In all
198 conditions, the sheet resistance is lower than the sheet resistance of SiC, but only C2 sample presents
199 properties consistent with graphene. The high sheet resistance presented by C1 and C3 may have
200 occurred because the “islands” of graphene produced are small and not interconnected. Both Raman
201 maps and AFM surface morphology images can endorse this fact.

202

203

204 **Table 2.** Sheet resistance of SiC thin film and graphene inferred by the four points probe method.

	C1	C2	C3	SiC ¹
Sheet resistance (Ω/\square)	30900	26	29320	60000

205 ¹ Reference measurement made on SiC film substrate.

206

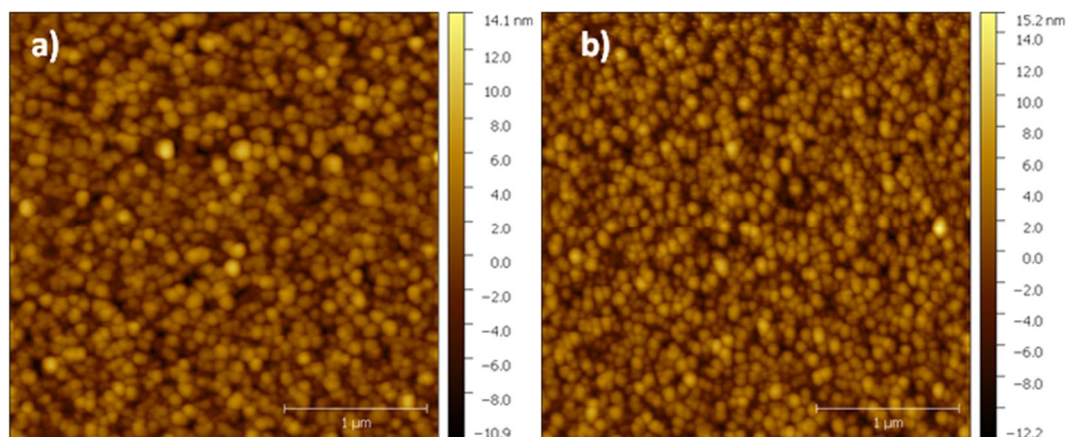
207

208 Before analyzing the surface morphology of the treated samples, it is important to verify the

209 morphology of the SiC surface. Figure 6 shows the AFM images of the surface of the SiC films and

210 the AlN buffer layer before laser treatment. As can be noticed, the SiC film follows the morphology

211 of the AlN layer with grains than 100 nm. These results indicate high quality SiC and AlN thin films.



212

213 **Figure 6.** Atomic force microscopy images of SiC (a) and AlN (b) films.

214

215 Figure 7 shows the surface morphology of the samples C1, C2 and C3. For samples C1 and C3

216 (Figures 7a and 7b), it is only possible to observe small isolated graphene islands. On the other hand,

217 for the sample C2 (Figures 7c and 7d), the graphene layers are larger and well distributed on surface

218 area in comparison with C1 and C3. The growth of the "islands" can be visualized in the profile of

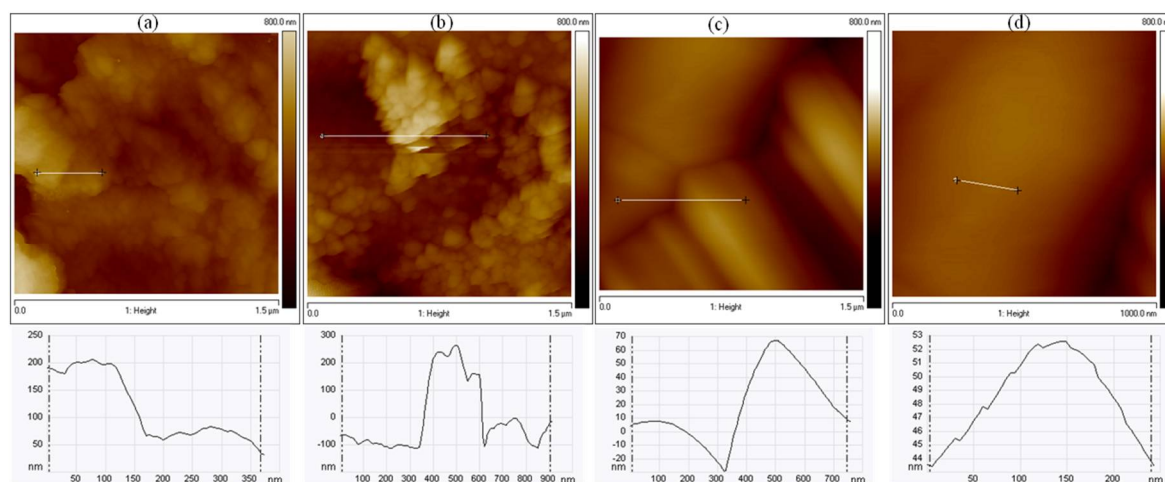
219 Figure 7d (sample C2), where stacking of the multilayers can be easier perceived. This result indicates

220 that even a small difference of the energy density of the CO₂ laser has a strong influence on the

221 quality of graphene grown on SiC film, which allows for the control of up to 3 orders of magnitude

222 of material resistivity.

223



224

225 **Figure 7.** Atomic force microscopy images of samples C1 (a); C3 (b); and C2 (c, d). White line =

226 profile traced to check the stacking of islands whose result is shown in the chart below each

227 image.

228

229 5. Conclusions

230 Herein, for the first time, we approached a feasible route for graphene growing based on the
231 thermal decomposition of polycrystalline SiC thin films deposited by HiPIMS technique on AlN/Si
232 substrates. For this purpose, we used a CO₂ laser beam heating without vacuum or controlled
233 atmosphere. Raman mapping along with AFM measurements revealed the formation of islands of
234 graphene on the SiC surfaces. The quality and density of graphene islands showed to be strongly
235 dependent on the energy density of laser process. It was observed that an energy density of the order
236 of 137 J cm⁻² allowed for the obtaining of graphene layers interconnected but with some defects along
237 the surface, resulting in a sheet resistance characteristic of graphene grown on pure crystal SiC wafer.
238 Conversely, when the energy density was increased to 145 J cm⁻², the density of defects was
239 considerably reduced. Finally, the results of this work demonstrate the feasibility of using the laser
240 beam technique as a heating source for graphene formation from SiC thin films, as well as give rise
241 to new possibilities to explore the development of graphene layers on different substrates using the
242 same methodology proposed here.

243

244 **Author Contributions:** N. G., G. V., R. P., J. M., M. G. and J. C. provide the investigation and methodology, N.
245 G., R. P., M. F., B. R., M. D. and H. M. white the original draft.

246 **Funding:** This work was supported by the Brazilian funding agencies: Coordenação de Aperfeiçoamento de
247 Pessoal de Nível Superior (CAPES), grants No. 23038.005802/2014-98 and No. 88881.064970/2014-01, Conselho
248 Nacional de Desenvolvimento Científico e Tecnológico (CNPq), grants No 473043/2012 and 301982/2015-5, and
249 Fundação de Amparo à Pesquisa do Estado de São Paulo (FAPESP), grants No. 2011/07468-2, 2018/01265-1 and
250 (FAPESP/CNPq/PRONEX) 2011/50773-0.

251 **Acknowledgments:** We gratefully acknowledge the Associate Laboratory of Sensors and Materials, Instituto
252 Nacional de Pesquisas Espaciais (INPE), for Raman measurements.

253 **Conflicts of Interest:** The authors declare no conflict of interest.

254 References

- 255 [1] R. Tu, Y. Liang, C. Zhang, J. Li, S. Zhang, M. Yang, Q. Li, T. Goto, L. Zhang, J. Shi, H. Li, H. Ohmori, M.
256 Kosinovas, B. Basu, Fast Synthesis of High-Quality Large-area Graphene by Laser CVD, *Applied Surface Science*
257 445 (2018) 204-210
- 258 [2] J. Hwang, M. Kim, V. B. Shields, M. G. Spencer, CVD growth of SiC on sapphire substrate and graphene
259 formation from the epitaxial SiC, *Journal of Crystal Growth* 366 (2013) 26-30.
- 260 [3] C. E. Giusca, S. J. Spencer, A. G. Shard, R. Yakimova, O. Kazakova, Exploring graphene formation on the C-
261 terminated face of SiC by structural, chemical and electrical methods, *Carbon* 69 (2014) 221-229.
- 262 [4] W. J. Ong, E. S. Tok, Role of Si clusters in the phase transformation and formation of (6×6)-ring structures on
263 6H-SiC(0001) as a function of temperature: An STM and XPS study, *Physical Review B* 73 (2006) 045330.
- 264 [5] B. Gupta, M. Notarianni, N. Mishra, M. Shafiei, F. Iacopi, N. Motta, Evolution of epitaxial graphene layers on
265 3C SiC/Si (111) as a function of annealing temperature in UHV, *Carbon* 68 (2014) 563-572.
- 266 [6] W. A. Heer, C. Berger, X. Wu, F. N. First, E. H. Conrad, X. Li, et al., Epitaxial graphene. *Solid State*
267 *Communications* 143 (2007) 92-100.
- 268 [7] J. Röhr, M. Hundhausen, K. V. Emtsev, Th. Seyller, R. Graupner, L. Ley, Raman spectra of epitaxial graphene
269 on SiC(0001). *Applied Physics Letters* 92 (2008) 201918-3.
- 270 [8] J. Tang, C. Y. Kang, L. M. Li, H. B. Pan, W. S. Yan, S. Q. Wei, et al., Graphene grown on sapphire surface by
271 using SiC buffer layer with SSMBE. *Physics Procedia*. 32 (2012) 880-884.
- 272 [9] A. B. G. Trabelsi, A. Ouerghi, O. E. Kusmartseva, F. V. Kusmartsev, M. Oueslati, Raman spectroscopy of four
273 epitaxial graphene layers: Macro-island grown on 4H-SiC substrate and an associated strain distribution. *Thin*
274 *Solid Films*. 539 (2013) 377-383.

- 275 [10] W. Norimatsu, M. Kusunoki, Structural features of epitaxial graphene on SiC {0001} surfaces. *J. Phys. D:*
276 *Appl. Phys.* 47 (2014) 094017.
- 277 [11] P. Avouris, C. Dimitrakopoulos, Graphene: synthesis and application. *Materials Today.* 15(3) (2012) 86-97.
- 278 [12] R. Yakimova, T. Iakimov, G. R. Yazdi, C. Bouhafs, J. Eriksson, A. Zakharov, et al., Morphological and
279 electronic properties of epitaxial graphene on SiC. *Physica B: Condensed Matter* 439 (2014) 54-59.
- 280 [13] D. Perrone, G. Maccioni, A. Chiolerio, C. M. Marigorta, M. Naretto, P. Pandolfi, et al., Study on the possibility
281 of graphene growth on 4H-silicon carbide surfaces via laser processing, Proceedings of the Fifth International
282 WLT-Conference on Lasers in Manufacturing (2009).
- 283 [14] S. Lee, M. F. Toney, W. Ko, J. C. Randel, H. J. Jung, K. Munakata, et al., Laser-Synthesized Epitaxial
284 Graphene. *ACS Nano* 12 (2010) 7524-7530.
- 285 [15] S. N. Yannopoulos, A. Siokou, N. K. Nasikas, V. Dracopoulos, F. Ravani, G. N. Papatheodorou, CO₂-Laser-
286 Induced Growth of Epitaxial Graphene on 6H-SiC(0001). *Advanced Functional Materials* 22 (2012) 113-120.
- 287 [16] M. A. Fraga, R. S. Pessoa, H. S. Maciel, M. Massi (2011). Recent Developments on Silicon Carbide Thin Films
288 for Piezoresistive Sensors Applications, Silicon Carbide - Materials, Processing and Applications in Electronic
289 Devices, Dr. Moumita Mukherjee (Ed.), InTech, DOI: 10.5772/20332. Available from:
290 [http://www.intechopen.com/books/silicon-carbide-materials-processing-and-applications-in-electronic-](http://www.intechopen.com/books/silicon-carbide-materials-processing-and-applications-in-electronic-devices/recent-developments-on-silicon-carbide-thin-films-for-piezoresistive-sensors-applications)
291 [devices/recent-developments-on-silicon-carbide-thin-films-for-piezoresistive-sensors-applications](http://www.intechopen.com/books/silicon-carbide-materials-processing-and-applications-in-electronic-devices/recent-developments-on-silicon-carbide-thin-films-for-piezoresistive-sensors-applications)
- 292 [17] M. A. Fraga, H. Furlan, R. S. Pessoa, L. A. Rasia, C. F. R. Mateus, Studies on SiC, DLC and TiO₂ thin films as
293 piezoresistive sensor materials for high temperature application, *Microsystem technologies* 18 (7-8) (2012) 1027-
294 1033.
- 295 [18] N. K. A. M. Galvão, G. Vasconcelos, M. V. R. dos Santos, T. M. B. Campos, R. S. Pessoa, M. Guerino, et al.,
296 Growth and Characterization of Graphene on Polycrystalline SiC Substrate Using Heating by CO₂ Laser Beam.
297 *Materials Research* 26 (2016) 1329-1334.
- 298 [19] R. Kumar, R. K. Singh, D. P. Singh, E. Joanni, R. M. Yadav, S. A. Moshkalev, Laser-assisted synthesis,
299 reduction and micro-patterning of graphene: Recent progress and applications, *Coordination Chemistry Reviews*
300 342 (2017) 34-79
- 301 [20] H. S. Medeiros, R. S. Pessoa, J. C. Sagas, M. A. Fraga, L. V. Santos, H. S. Maciel, et al., Effect of nitrogen
302 content in amorphous SiC_xN_yO_z thin films deposited by low temperature reactive magnetron co-sputtering
303 technique. *Surface & Coatings Technology*, 206 (2011) 1787-1795.
- 304 [21] B. E. Belkerk, A. Sousou, M. Carette, M. A. Djouadi, Y. Scudeller, Structural-dependent thermal
305 conductivity of aluminium nitride produced by reactive direct current magnetron sputtering, *Applied Physics*
306 *Letters* 101 (2012) 151908.
- 307 [22] A. Eckmann, A. Felten, A. Mishchenko, L. Britnell, R. Krupke, K. S. Novoselov, et al., Probing the Nature of
308 Defects in Graphene by Raman Spectroscopy, *NanoLetters*, 12 (2012) 3925-3930.
- 309 [23] G. Leal, T. M. B. Campos, A. S. da Silva Sobrinho, R. S. Pessoa, H. S. Maciel, M. Massi, Characterization of
310 SiC thin films deposited by HiPIMS. *Materials Research* 17(2) (2014) 472-476.
- 311 [24] K. A. Aissa, A. Achour, J. Camus, L. Le Brizoual, P.-Y. Jouan, M.-A. Djouadi, Comparison of the structural
312 properties and residual stress of AlN films deposited by dc magnetron sputtering and high power impulse
313 magnetron sputtering at different working pressures, *Thin Solid Films* 550 (2014) 264-267.
- 314 [25] W. Li, J. Yuan, Y. Lin, S. Yao, Z. Ren, H. Wang, et al., The controlled formation of hybrid structures of multi-
315 walled carbon nanotubes on SiC plate-like particles and their synergetic effect as a filler in poly(vinylidene
316 fluoride) based composites, *Carbon* 51 (2013) 355-364.

- 317 [26] K. Raju, H. W. Yu, J. -Y. Park, D. H. Yoo, Fabrication of SiCf/SiC composites by alternating current
318 electrophoretic deposition (AC-EPD) and hot pressing, *Journal of the European Ceramic Society* 35 (2015) 503-511.
- 319 [27] K. J. Kim, M. H. Kim, Y. -W. Kim, Highly Conductive p-Type Zinc blende SiC Thin Films Fabricated on
320 Silicon Substrates by Magnetron Sputtering, *J. Am. Ceram. Soc.* 98 (12) (2015) 3663-3665.
- 321 [28] I. Calizo, I. Bejenari, M. Rahman, G. Liu, A. A. Balandin, Ultraviolet Raman microscopy of single and
322 multilayer graphene, *Journal of Applied Physics* 106 (2009) 043509.
- 323 [29] L. G. Cançado, K. Takai, T. Enoki, General equation for the determination of the crystallite size L_a of
324 nanographite by Raman spectroscopy. *Appl. Phys. Lett.* 88 (2006) 163-166.
- 325 [30] M. A. Pimenta, G. Dresselhaus, M. S. Dresselhaus, L. G. Cançado, A. Jorio, R. Saito, Studying disorder in
326 graphite-based systems by Raman spectroscopy. *Phys. Chem. Chem. Phys.* 9(11) (2007) 1276-1291.
- 327 [31] L. M. Malard, M. A. Pimenta, G. Dresselhaus, M. S. Dresselhaus, Raman spectroscopy in graphene. *Phys.*
328 *Rep.* 473 (5-6) (2009) 51-87.
- 329 [32] B. Kumar, M. Baraket, M. Paillet, J. -R. Huntzinger, A. Tiberj, A. G. M. Jansen, et al., Growth protocols and
330 characterization of epitaxial graphene on SiC elaborated in a graphite enclosure, *Physica E* 75 (2016) 7-14.
- 331 [33] E. Escobedo-Cousin, K. Vassilevski, T. Hopf, N. Wright, A. O'Neill, A. Horsfall, et al., Local solid phase
332 growth of few-layer graphene on silicon carbide from nickel silicide supersaturated with carbon. *Journal of*
333 *Applied Physics* 2013, 113(11), 114309.
- 334 [34] J. Hass, W. A. de Heer, E. H. Conrad, The growth and morphology of epitaxial multilayer graphene, *J. Phys.:*
335 *Condens. Matter* 20 (2008) 323202 (27pp)
- 336 [35] A. Tiberj, N. Camara, P. Godignon, J. Camassel, Micro-Raman and micro-transmission imaging of epitaxial
337 graphene grown on the Si and C faces of 6H-SiC, *Nanoscale Research Letters* (2011), 6:478
- 338 [36] G. G. Jernigan, B. L. VanMil, J. L. Tedesco, J. G. Tischler, E. R. Glaser, A. Davidson III, et al., Comparison of
339 Epitaxial Graphene on Si-face and C-face 4H SiC Formed by Ultrahigh Vacuum and RF Furnace Production,
340 *Nano Lett.* 9 (7) (2009) 2605-2609.
- 341 [37] J. Hass, R. Feng, T. Li, X. Li, Z. Zong, W. A. de Heer, et al., Highly ordered graphene for two dimensional
342 electronics *Appl. Phys. Lett.* 89 (2006) 143106.
- 343
- 344